Precision Luminosity of LHC Proton–Proton Collisions at 13 TeV Using Hit Counting With TPX Pixel Devices

André Sopczak, *Senior Member, IEEE*, Babar Ali, Thanawat Asawatavonvanich, Jakub Begera, Benedikt Bergmann, Thomas Billoud, Petr Burian, Ivan Caicedo, Davide Caforio, Erik Heijne, *Fellow, IEEE*, Josef Janeček, Claude Leroy, *Member, IEEE*, Petr Mánek, Kazuya Mochizuki, Yesid Mora, Josef Pacík, Costa Papadatos, Michal Platkevič, Štěpán Polanský, Stanislav Pospíšil, *Senior Member, IEEE*, Michal Suk, and Zdeněk Svoboda

***Abstract*— A network of Timepix (TPX) devices installed in the ATLAS cavern measures the LHC luminosity as a function of time as a stand-alone system. The data were recorded from 13-TeV proton–proton collisions in 2015. Using two TPX devices, the number of hits created by particles passing the pixel matrices was counted. A van der Meer scan of the LHC beams was analyzed using bunch-integrated luminosity averages over the different bunch profiles for an approximate absolute luminosity normalization. It is demonstrated that the TPX network has the capability to measure the reduction of LHC luminosity with precision. Comparative studies were performed among four sensors (two sensors in each TPX device) and the relative short-term precision of the luminosity measurement was determined to be 0.1% for 10-s time intervals. The internal long-term time stability of the measurements was below 0.5% for the data-taking period .**

***Index Terms*— Colliding beam accelerators, LHC, luminosity, Timepix.**

I. Introduction

A TPX detector network [1] of 16 devices was installed in the ATLAS cavern at CERN. Each TPX device consists of two stacked hybrid silicon pixel sensors. The silicon sensors have a matrix of 256 × 256 pixels of 55-μm pitch and the thicknesses of 300 μm (further indicated as layer-1) and 500 μm (layer-2) [2]. The readout chips connected to these sensors have the original TPX design [3], [4]. The installation of the TPX devices took place during the LHC shutdown transition from Run-1 to Run-2 in 2013/2014. These double-layer TPX devices replaced the previously operational network that employed single-layer Medipix (MPX) assemblies [5], [6].

These devices measure the primary and secondary particle fluxes resulting from 13-TeV proton–proton collisions. The data were taken in 2015 during the first year of LHC Run-2 operation. Precision luminosity measurements are of particular importance for many physics analyses in high-energy physics.

The use of the TPX network for luminosity measurements has several advantages compared with the previous luminosity measurements [7] at LHC during Run-1 that used MPX devices. Regarding the luminosity monitoring, the two-layer hodoscope structure of the TPX devices doubles the measurement statistics and allows one to determine the precision and long-term time stability of individual TPX devices. The dead time caused by the readout was reduced from about 6 to 0.12 s allowing a much higher data acquisition rate. Also, the TPX devices are operated in three different modes [3], [4]: 1) hit counting; 2) time-over-threshold (energy deposits and cluster-counting); and 3) time-of-arrival (cluster counting). Furthermore, the proton–proton collision energy increased from 8 TeV at LHC during Run-1 to 13 TeV at Run-2, which opened a new energy frontier for luminosity measurements in colliders.

The TPX network is self-sufficient for luminosity monitoring. It collects data independently of the ATLAS data-recording chain and provides independent measurements of the bunch-integrated LHC luminosity. In particular, van der Meer (vdM) scans [8] can be used for absolute luminosity calibration.

The detection of charged particles in the TPX devices is based on the ionization energy deposited by particles passing through the silicon sensor. The signals are processed and digitized during an adjustable exposure time (frame acquisition time) for each pixel. Neutral particles, namely neutrons, however, need to be converted into charged particles before they can be detected. Therefore, a part of each silicon sensor is covered by ^{6}LiF and polyethylene converters [2], [9].

Manuscript received November 6, 2016; accepted January 29, 2017. Date of publication February 6, 2017; date of current version March 30, 2017. This work was supported in part by the Ministry of Education, Youth and Sports of the Czech Republic under Project LG 15052 and Project LM 2015058, in part by the Natural Sciences and Engineering Research Council of Canada, and in part by the Prague Van-de-Graaff Accelerator funded by the Ministry of Education, Youth and Sports of the Czech Republic under Project LM 2015077.

A. Sopczak, B. Ali, T. Asawatavonvanich, J. Begera, B. Bergmann, P. Burian, I. Caicedo, D. Caforio, E. Heijne, J. Janeček, P. Mánek, Y. Mora, J. Pacík, M. Platkevič, S. Polanský, S. Pospíšil, M. Suk, and Z. Svoboda are with the Institute of Experimental and Applied Physics, Czech Technical University in Prague, Prague CZ-128 00, Czech Republic (e-mail: andre.sopczak@cern.ch).

T. Billoud, C. Leroy, K. Mochizuki, and C. Papadatos are with the Group of Particle Physics, University of Montreal, Montréal, QC H3T 1J4T, Canada.

Color versions of one or more of the figures in this paper are available online at http://ieeexplore.ieee.org.

Digital Object Identifier 10.1109/TNS.2017.2664664

TABLE I

TPX DEVICE LOCATIONS WITH RESPECT TO THE INTERACTION POINT. Z IS THE LONGITUDINAL DISTANCE FROM THE INTERACTION POINT AND R IS THE DISTANCE FROM THE BEAM AXIS. THEIR UNCERTAINTY IS ABOUT 10 mm

Device	Z (mm)	R (mm)	TPX clusters per unit sensor area and per unit luminosity ($\mathrm{cm}^{-2}/\mathrm{nb}^{-1}$)	
			Layer-1	Layer-2
TPX02	3540	1115	104	123
TPX12	-3540	1146	97	113

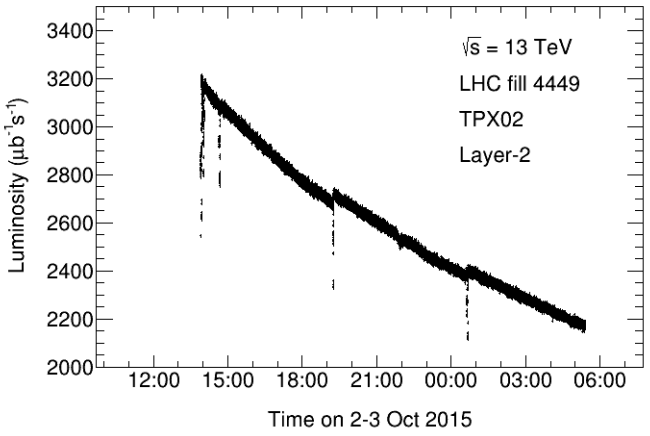

Fig. 1. Time history of the TPX luminosity. The small dips, visible as variations from the descending curve, correspond to the times when the LHC operators performed small-amplitude beam separation scans to optimize the luminosity. The normalization between hit rate and luminosity is based on vdM scans using LHC fill 4266, as detailed in Section III.

Thirteen out of the sixteen installed devices have been used for the luminosity analysis. Two devices were found to be inoperational after the closing of the ATLAS detector and one device was intentionally located far away from the interaction point, and therefore, it was unusable for luminosity measurements. Table I lists the locations of the devices TPX02 and TPX12 used in this analysis and their numbers of registered passing particles (clusters). It is noted that the number of clusters of the 500-μm sensor is about 20% larger compared with that of the 300-μm sensor. This percentage is lower than might be expected from the 40% larger sensitive volume, because the extended clusters induced by a single particle count only "one" in the thin as well as in the thick sensor. The number of photon conversions and fast neutron interactions, however, will increase with the sensitive volume. The analysis described in this paper is focused on the precision luminosity determination with the devices TPX02 and TPX12, which are operated with a 1-s exposure time and analyzed in hit counting mode. As their positions are very similar in R and Z coordinates on opposite sides of the proton–proton interaction point, their count rates are very similar. During 2015, LHC proton–proton collisions typical luminosities were $\mathcal{L} = 3\text{–}5 \times 10^{33}\ \mathrm{cm}^{-2}\mathrm{s}^{-1} = 3000\text{–}5000\ \mu\mathrm{b}^{-1}\mathrm{s}^{-1}$ and the TPX count rate was a few 10^6 hits/s per frame.

Fig. 1 shows an example of the luminosity from hit counting measured with TPX02 layer-2 for LHC fill 4449, taken on October 2–3, 2015. All times are in GMT.

This paper is structured as follows. First, the concept of LHC luminosity monitoring from TPX hit counting is introduced in Section II. The vdM scan analysis based on hit counting (Section III) is summarized for an absolute luminosity calibration. In Section IV, the LHC luminosity curve is determined by using the concept of averaged interactions per bunch crossing together with the TPX measurement precision. Section V describes the luminosity precision by evaluation of the difference between two layers of the same TPX device. The long-term luminosity precision is given in Section VI from the comparison of layer-1 and layer-2 luminosity of the same TPX device. The long-term luminosity precision from different TPX devices is given in Section VII. Finally, conclusions are given in Section VIII.

II. LHC LUMINOSITY FROM TPX HIT COUNTING

The data from the TPX02 and TPX12 devices were used in hit counting mode, both having similar count rates as specified in Table I. The devices measure the luminosity independently and their measurements are cross checked with each other. A constant exposure time of 1 s was used for the entire 2015 data taking.

A small number of pixels becoming weak or noisy (e.g., due to radiation damage) could have a significant effect on the luminosity measurement. Therefore, pixels with a count rate that is at least 3σ away from the mean are excluded for each sensor region (uncovered and with converters). This requirement identifies about 7%–13% of the pixels on layer-1 and layer-2 both for TPX02 and TPX12 per LHC fill, including 5%–10% of pixels at the boundaries of the sensor regions and edges of the sensor matrix. Then, the logical OR of identified pixels per LHC fill was taken for all 2015 LHC fills to remove 19%–22% of the total number of pixels of the sensors. The effect of the pixel removal on the analysis was also studied with 2σ and 5σ criteria, with the result that the analysis outcome regarding the LHC luminosity curve, measurement precision, and long-term stability remained unchanged.

The hit rate for the four TPX sensors is normalized to units of luminosity by multiplying with a scaling factor, as given in Section III.

The induced radioactivity of material in the ATLAS cavern has no significant effect on the luminosity determination as determined by a dedicated study.

The ATLAS and CMS collaborations have elaborate systems of luminosity measurements, as described in [10] and [11] (ATLAS) and [12] and [13] (CMS). A comparative study of their results and the TPX luminosity monitoring is beyond the scope of this paper.

In addition to the hit counting, luminosity can be measured with the two other modes of TPX operation based on cluster-counting and summed energy deposits. These luminosity measurements will be addressed in a separate publication.

The relation between the number of hits and clusters (particles) is investigated in order to determine the statistical uncertainty of the luminosity measurement from hit counting. The average ratio of hits per cluster is approximately $R = N_{\mathrm{hit}}/N_{\mathrm{cl}} = 10$, which was obtained with TPX data

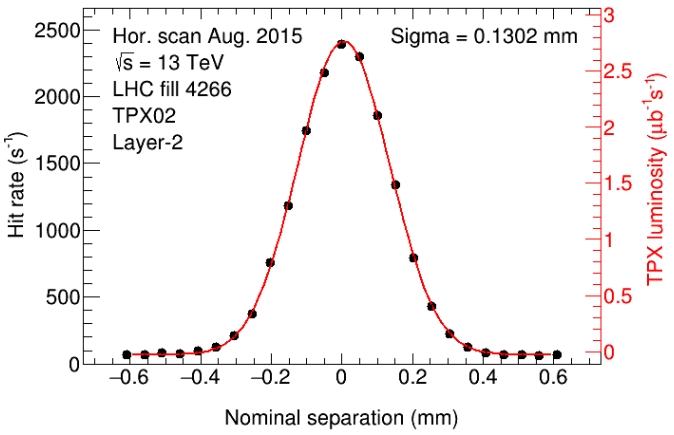

Fig. 2. Luminosity from hit counting as a function of nominal beam separation measured with TPX02 layer-2 during the first horizontal vdM scan in August 2015. Each data point shows the measured instantaneous luminosity before background subtraction. Because the exposure time is significantly shorter than the duration of a scan step, the TPX samplings are averaged per scan step. The TPX samplings that partially or totally overlap with nonquiescent scan steps (varying beam separation) are not shown. The fit function is the sum of a single Gaussian (representing the proper luminosity in this scan) and a constant term that accounts for instrumental noise and single-beam background. The TPX normalization uses this horizontal and a vertical beam width from LHC vdM fill 4266.

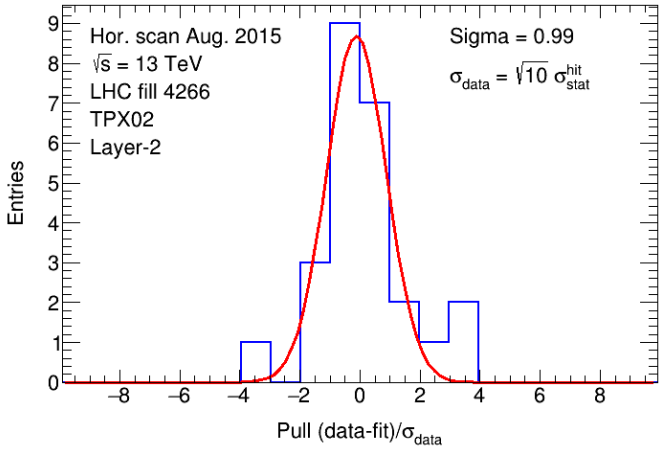

Fig. 3. Pull distribution defined as (data-fit)/σ_{data}, where $\sigma_{\text{data}} = \sqrt{R} \cdot \sigma_{\text{stat}}^{\text{hit}}$, with $R = N_{\text{hit}}/N_{\text{cl}} = 10$ for TPX02 layer-2. The data shown in Fig. 2 are used. LHC fill 4266.

from a low-intensity LHC fill for which the clusters on the sensors were well separated. This factor is used for the statistical uncertainty determination in the following sections assuming that one cluster corresponds to one independent particle passing the device [7].

III. Van Der Meer Scans

vdM scans are used for absolute luminosity calibration at the LHC. This scan technique was pioneered by Simon vdM at CERN in the 1960s [8] to determine the luminosity calibration in a simple way. It involves scanning the LHC beams through one another to determine their sizes in terms of the horizontal and vertical widths of the beams at the point of collision. These width measurements are then combined with information of the number of circulating protons, allowing the determination of an absolute luminosity scale. The vdM scan analysis is based on the data taken on August 24, 2015 and August 25, 2015 using TPX02 and TPX12 layer-1 and layer-2.

The LHC beam separation dependence of the measured TPX luminosity is well represented by the sum of a single Gaussian and a constant (Fig. 2). The absolute luminosity normalization is derived from the combination of the hit rate, the horizontal and vertical convoluted widths, and the average bunch currents.

The measurement uncertainty of the TPX devices can be determined with respect to the expected statistical uncertainty. For this study, the pull distributions, as defined by (data-fit)/σ_{data}, were determined, where $\sigma_{\text{data}} = \sqrt{R} \cdot \sigma_{\text{stat}}^{\text{hit}}$, $\sigma_{\text{stat}}^{\text{hit}} = \text{data}/\sqrt{N_{\text{hit}}}$, and $R = 10$. Fig. 3 shows the pull distribution for the first horizontal vdM scan in August 2015, as seen by TPX02 layer-2. The sigma of the pull distribution averaged over TPX02 and TPX12, layer-1 and layer-2 for both horizontal and vertical scans, is 2.0 ± 0.6, which indicates that additional uncertainties are present beyond the determined statistical uncertainties or correlations in the statistical evaluation have a significant effect as discussed in [7]. Furthermore, transverse proton-bunch profiles are not expected to be perfectly Gaussian; and even if they were, a scan curve summed over Gaussian bunches of different widths would not be strictly Gaussian. Therefore, non-Gaussian contributions to the vdM-scan curves may contribute, at some level, to the widening of the pull distribution.

For TPX02 layer-2, the widths of the beam sizes (horizontal and vertical nominal beam separations) and their statistical uncertainties are $\Sigma_x = (130.2 \pm 0.5)\mu\text{m}$ and $\Sigma_y = (118.6 \pm 0.5)\mu\text{m}$, respectively.

The luminosity can be calculated as

$$L_{\text{TPX}} = N_b N_{p1} N_{p2} f/(2\pi\, \Sigma_x\, \Sigma_y) \tag{1}$$

where N_b is the number of bunch crossings producing collisions per machine revolution, N_{p1} and N_{p2} are the average bunch populations (number of protons) in beam 1 and beam 2, respectively, f is the machine revolution frequency (11 245.5 Hz), and Σ_x and Σ_y are the convoluted horizontal and vertical beam sizes. The LHC parameters for fill 4266 are as follows [14]:

1) the number of bunches: $N_b = 30$;
2) the average number of protons (in units 10^{11}) per bunch in beam 1 and in beam 2: $N_{p1} = 26.5/30 = 0.883$ and $N_{p2} = 26.6/30 = 0.887$, respectively.

Thus, the resulting luminosity is $L_{\text{TPX}} = 2.724\mu\text{b}^{-1}\text{s}^{-1}$.

The specific luminosity is defined as

$$L_{\text{specific}} = L_{\text{TPX}}/(N_b N_{p1} N_{p2}) = f/(2\pi\, \Sigma_x\, \Sigma_y). \tag{2}$$

Table II summarizes the scan results for the first pair of vdM scans (horizontal and vertical) registered with TPX02 and TPX12 for both their layers.

For TPX02 layer-2, the fits of horizontal and vertical scans provide (2357 ± 14) and (2415 ± 16) hits/s, respectively, at the peak above the background. The average number is (2386 ± 11) hits/s. Thus, the normalization factor n_f between the TPX02 layer-2 hit rate and the instantaneous

TABLE II

vdM SCAN RESULTS FOR 2015 DATA. THE SCAN WAS PERFORMED ON AUGUST 24 AND AUGUST 25 (LHC FILL 4266) AND THE FIRST HORIZONTAL AND VERTICAL SCANS WERE USED. THE FIT RESULTS FOR THE FIRST BUNCH-AVERAGED HORIZONTAL Σ_x AND VERTICAL Σ_y CONVOLUTED BEAM SIZES ARE GIVEN, AS WELL AS THE SPECIFIC LUMINOSITY. THE HIT RATE AT THE PEAK IS AVERAGED OVER THE HORIZONTAL AND VERTICAL SCANS

TPX	Layer	Σ_x (μm)	Σ_y (μm)	L_{specific} ($\mu b^{-1}s^{-1}/10^{25}$)	N_{peak} (hits/s)
02	1	130.2	117.7	116.8	1495
02	2	130.2	118.6	115.9	2386
12	1	128.7	118.1	117.8	1386
12	2	128.3	118.7	117.5	2298

TABLE III

NORMALIZATION ($1/n_f$) TO CONVERT HIT RATES INTO LUMINOSITIES. THE LARGER VALUES ARE FOR THE THICKER SENSOR LAYER

Device	Layer	$1/n_f$ (hits/μb^{-1})
TPX02	1	544.8
TPX02	2	876.1
TPX12	1	500.9
TPX12	2	832.2

LHC luminosity is

$$n_f = \frac{2.724 \mu b^{-1} s^{-1}}{2386 \text{hit s}^{-1}} = 1.141 \cdot 10^{-3} \ \mu b^{-1}/\text{hit}. \quad (3)$$

The normalization factors for the other devices were calculated using the same procedure, and the results are summarized in Table III.

As already noted for the previous LHC Run-1 vdM scan analysis using MPX devices [7], the normalization factor for the absolute luminosity is only approximate since the TPX exposure time is much longer than the bunch spacing. Therefore, the bunch-integrated luminosity averages over the different bunch profiles. In order to estimate the resulting uncertainty, a simulation with 29 overlapping Gaussian distributions was performed [7], which led to an estimate of the resulting uncertainty on the normalization factor (from this source only) of about 1%.

Although further uncertainties could arise from non-Gaussian shapes, this paper shows that the Gaussian approximation of the sum of Gaussians is quite robust with the TPX system and the luminosity approximation by bunch integration is a sensible approach. No attempt was made for a precise determination of the total uncertainty, which would require a dedicated study [10], [11].

IV. LHC LUMINOSITY CURVE AND TPX PRECISION

The TPX network has the capability to study the LHC luminosity curve with precision. Six LHC fills of proton–proton collisions were investigated in detail. As an example, details are given for the LHC fill 4449, taken on October 3, 2015.

First, the TPX luminosity is calculated using the normalization factors from Table III and it is then converted into an average number of inelastic interactions per bunch crossing by

$$\mu = L \cdot \sigma_{\text{inel}}/(N_b \cdot f) \quad (4)$$

where $N_b = 1453$ colliding bunches, $f = 11245.5$ Hz, and the inelastic cross section $\sigma_{\text{inel}} = 80$ mb [15]. Accelerator simulations [16] have shown that under routine physics conditions ($\beta^* < 1$ m), elastic proton–proton scattering contributes negligibly to the particle loss rate. This is because the typical scattering angle is so small compared with the natural angular divergence of the beam that the protons remain with the dynamic aperture of the ring.

A. Fitted LHC Luminosity Curve

In a simple approximation, the loss rate of protons N in the colliding beam is governed by

$$-dN/dt = \lambda_{bb} N^2/N_0 + \lambda_g N \quad (5)$$

where N_0 is the initial number of protons and λ_{bb} and λ_g are constants related to beam–beam (burning off the proton bunches) and single-bunch (e.g., beam–gas) interactions, respectively. This equation has a known solution, which is used as a fit function

$$N(t) = \frac{N_0 e^{-\lambda_g t}}{1 + \frac{\lambda_{bb}}{\lambda_g}(1 - e^{-\lambda_g t})} \quad (6)$$

with two well-known border cases

$$N(t) = N_0 e^{-\lambda_g t} \quad \text{for } \lambda_{bb} \ll \lambda_g \quad (7)$$

and

$$N(t) = \frac{N_0}{1 + \lambda_{bb} t} \quad \text{for } \lambda_g \ll \lambda_{bb}. \quad (8)$$

Next, the expected mean lifetime of inelastic beam–beam interactions is calculated from the LHC beam parameters, as given in Table IV, and used as a fixed parameter to determine λ_g. A simultaneous fit of λ_{bb} and λ_g did not converge. As already noted in the previous LHC Run-1 analysis [7], λ_{bb} and λ_g are strongly anticorrelated. Compared with the data taking at Run-1, the Run-2 LHC luminosity curve is flatter, making the fit less sensitive to the fit parameters.

The mean lifetime from inelastic beam-beam interactions is given by [17]

$$t_{bb}^{\text{inel}} = N_b N_0/(N_{\text{exp}} L_0 \sigma_{\text{inel}}) \quad (9)$$

where N_0 is the initial number of protons per bunch ($N_b N_0 = 1.6 \cdot 10^{14}$ protons [14]). For LHC fill 4440, the initial luminosity is $L_0 = 3360 \mu b^{-1} s^{-1}$ [14] and the number of experiments is $N_{\text{exp}} = 2$ (ATLAS [18] and CMS [19]). For the lifetime, $t_{bb}^{\text{inel}} = 3.07 \times 10^5$s is obtained, and thus

$$\lambda_{bb}^{\text{inel}} = 1/t_{bb}^{\text{inel}} = 0.2815 \text{ day}^{-1}. \quad (10)$$

The value $\lambda_{bb}^{\text{inel}}$ depends on the initial luminosity and the initial number of protons and thus on the starting value of $\mu_1 = 10.43$ for the first fit. Since $L \propto N^2$, one can write $\lambda_{bb}^{\text{inel}} \propto \sqrt{L_0} \propto \sqrt{\mu_0}$. Thus, for the lower initial luminosity

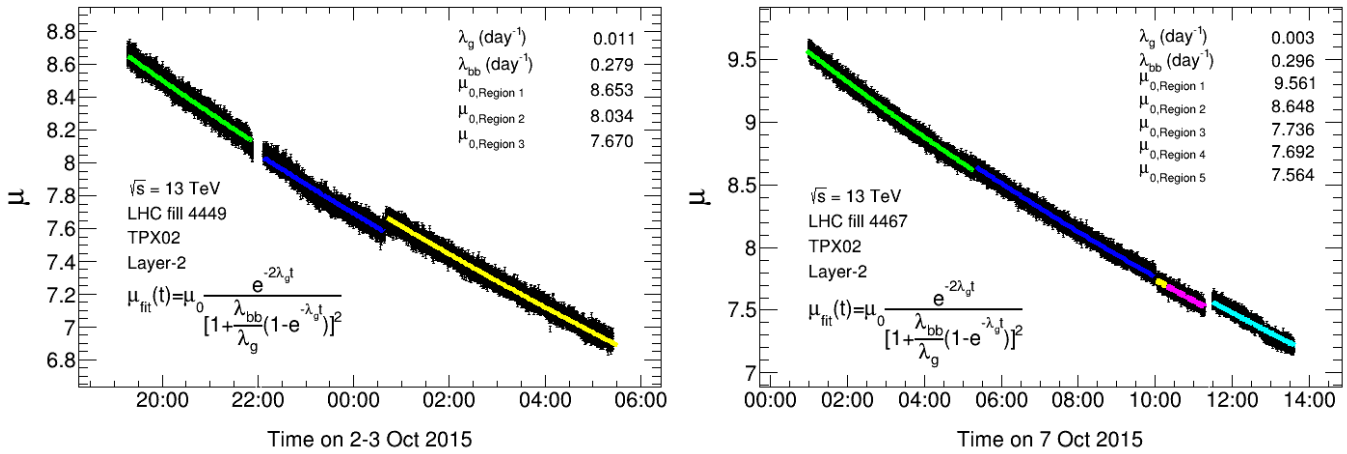

Fig. 4. Average number of interactions per bunch crossing as a function of time, seen by TPX02 layer-2 in hit counting mode. The distribution is approximately described by a function as given in the figure. The parameters are defined in the text. The statistical uncertainties per data point are indicated. They depend on the hit statistics scaled by a factor $\sqrt{10}$. For the first time intervals, the $\lambda_{\rm bb}$ is calculated analytically from the LHC parameters, and for the subsequent time intervals, $\lambda_{\rm bb}$ is scaled with $(\mu_i/\mu_1)^{1/2}$, where the index corresponds to the time period.

TABLE IV

PARAMETERS OF THE LHC PROTON–PROTON COLLISIONS FOR THE 2015 FILLS ANALYZED WITH TPX02 AND TPX12 IN THE FITTING OF LHC LUMINOSITY REDUCTION CURVE. L_0 IS THE LUMINOSITY AND μ_0 IS THE AVERAGE NUMBER OF INTERACTIONS PER BUNCH CROSSING AT THE START OF THE LHC FILL. THE $\lambda^0_{\rm bb}$ IS GIVEN FOR THE START OF THE LHC FILL, AND $\lambda^1_{\rm bb}$ IS GIVEN AT THE START TIME OF THE FIT FOR THE FIRST TIME PERIOD

Date in 2015	Fill	Start time (unix time)	kN_0 (10^{11})	L_0 ($\mu b^{-1}s^{-1}$)	μ_0	Colliding bunches	$\lambda^0_{\rm bb}$ (day^{-1})	$\lambda^1_{\rm bb}$ (day^{-1})
29 Sep.	4440	1443525360	1650	3360	24.8	1453	0.2815	0.1833
2-3 Oct.	4449	1443785520	1607	3240	26.0	1453	0.2787	0.1615
6-7 Oct.	4467	1444149360	1729	3700	24.1	1596	0.2958	0.1873
9-11 Oct.	4479	1444427640	1950	4240	24.6	1813	0.3006	0.2194
30-31 Oct.	4557	1446221040	2388	4450	24.7	2232	0.2576	0.1840
31 Oct.-1 Nov.	4560	1446311100	2610	5020	24.5	2232	0.2659	0.1859

in the fit, a longer lifetime is expected from beam–beam interactions and therefore a smaller

$$\lambda^1_{\rm bb} = \sqrt{10.51/24.8} \cdot 0.2815 \text{ day}^{-1} = 0.1833 \text{ day}^{-1}. \quad (11)$$

The frequent LHC small-amplitude beam separation scans for optimization of the luminosity made it necessary to adapt the fit function. Therefore, the data during the scans are removed and the LHC luminosity curve is fitted with a function having the values of $\lambda_{\rm bb}$ reduced by $(\mu_i/\mu_0)^{1/2}$ for each time period between the scans. The μ_i values are calculated for the starting values for each region between the scans, and μ_0 is the value for the start of the LHC fill.

Six long LHC fills with large luminosity are investigated as given in Table IV. Fig. 4 shows the fit of TPX02 layer-2 data for two of these LHC fills.

The fit results indicate that the LHC luminosity reduction is predominantly reduced by beam–beam interactions since a larger value of $\lambda_{\rm bb}$ corresponds to a shorter lifetime. In order to determine the $\lambda_{\rm g}$ and its uncertainty, the fit is performed for the six LHC fills and the four sensors separately, resulting in a large single-bunch lifetime $1/\lambda_{\rm g}$

$$\lambda^{\rm avg}_{\rm g} = (0.04 \pm 0.03) \text{ day}^{-1} \quad (12)$$

where the average is taken over 24 measurements and the uncertainty is given as the square root of the variance.

B. Precision

In order to investigate the precision of the TPX luminosity measurements, the difference between the fit and the data is studied as a function of time. As an example, the data are analyzed from the last continuous LHC curve taken on October 3, 2015 for about 4.5 h starting 0:45.

A precision of 0.35% has been obtained with TPX02 layer-2 and similarly with other TPX sensors, as listed in Table V. The given uncertainties result from statistical and systematic uncertainties by the TPX measurements convoluted with uncertainties arising from fluctuations in the proton–proton collision rates.

It is noted that the TPX measurement precision is statistically limited by the number of hits per frame. Therefore, 10, 20, 30, and 40 frames are grouped together. Consequently, the statistical precision significantly increases. Fig. 5 shows the residuals for groups of 30 frames. The four distributions show no particular uniform structure and therefore no LHC luminosity variation at the 0.1% level. Table V lists the obtained precisions for TPX02 and TPX12 layer-1 and layer-2. The fit results using the data of the four sensors are consistent.

TABLE V

PRECISION OF TPX02 AND TPX12 LUMINOSITY MEASUREMENTS FOR THE AVERAGE OF LAYER-1 AND LAYER-2. THE PRECISION IS GIVEN FOR 1 FRAME AND FOR 10, 20, 30, AND 40 FRAMES COMBINED. THE WIDTH OF THE GAUSSIAN FIT $\sigma_{(\mathrm{data-fit})/\mathrm{fit}}$ GIVES THE PRECISION OF THE MEASUREMENT AND σ_{pull} GIVES THE WIDTH OF THE FIT OF THE PULL DISTRIBUTION WITH STATISTICAL UNCERTAINTIES ONLY. LHC FILL 4449

Frames used	$\sigma_{(\mathrm{data-fit})/\mathrm{fit}}$ (%)				σ_{pull}			
	TPX02		TPX12		TPX02		TPX12	
	Layer-1	Layer-2	Layer-1	Layer-2	Layer-1	Layer-2	Layer-1	Layer-2
1	0.36	0.35	0.37	0.36	1.27	1.58	1.28	1.57
10	0.13	0.13	0.15	0.13	1.47	1.87	1.61	1.82
20	0.11	0.10	0.13	0.11	1.71	2.04	1.96	2.12
30	0.10	0.09	0.11	0.10	1.96	2.18	2.17	2.40
40	0.09	0.08	0.11	0.09	2.13	2.39	2.24	2.56

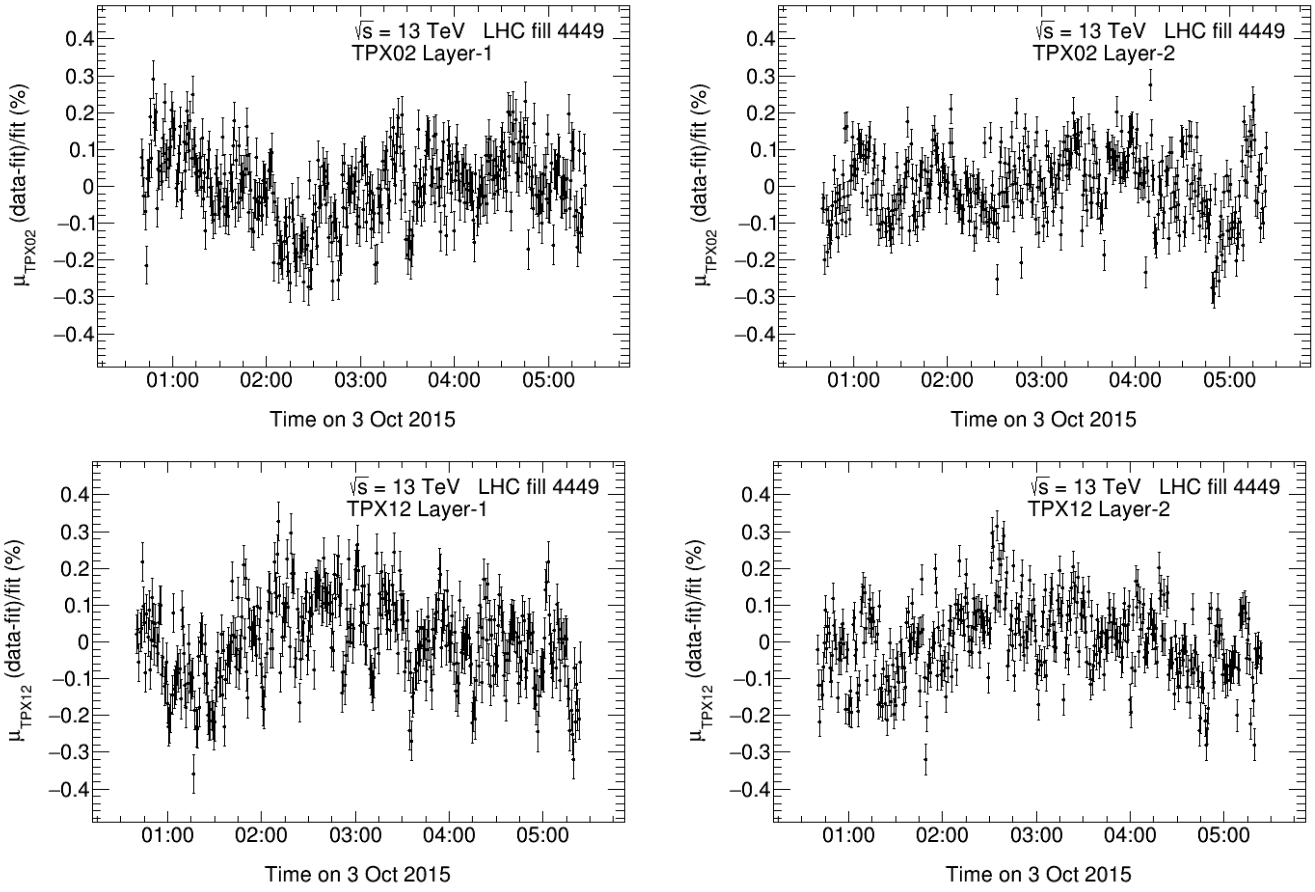

Fig. 5. Relative difference between the data and the fitted average number of interactions per bunch crossing as a function of time, seen by TPX02 and TPX12 for layer-1 and layer-2. The data are shown for 30 frames (1 s each) combined in order to decrease the statistical uncertainty. LHC fill 4449.

In order to increase the statistical significance of each TPX device, the luminosity measured by layer-1 and layer-2 is averaged and presented in Fig. 6 for ten frames combined. It shows the relative difference between the data and the fitted average number of interactions per bunch crossing as a function of time, seen by TPX02. The corresponding Gaussian fit is shown in Fig. 7. Fig. 8 shows the pull distribution assuming statistical uncertainties only. Table VI lists the obtained uncertainties and the corresponding pull values for 1 frame, as well as for 10, 20, 30, and 40 frames combined. The resulting relative short-term luminosity measurement precision is 0.1% for 10-s time intervals. As a consistency check of the obtained precision, the data from October 7, 2015 (LHC fill 4467) from 5:30 to 10:00 was analyzed in the same way, reproducing the results on the precision. Thus, the resulting luminosity precision of the TPX system is higher compared with the previous MPX luminosity measurement precision (0.3% for a 60-s time interval) [7] for data taken at LHC during Run-1 operation.

V. SHORT-TERM PRECISION OF INDIVIDUAL TPX DEVICES

In order to determine the short-term precision of individual TPX devices for luminosity measurements, the relative difference in luminosity measured by layer-1 and layer-2 of

TABLE VI

PRECISION OF TPX02 AND TPX12 LUMINOSITY MEASUREMENTS WITH RESPECT TO THE FITTED CURVE FOR THE AVERAGE OF LAYER-1 AND LAYER-2. THE PRECISION IS GIVEN FOR 1 FRAME AND FOR THE 10, 20, 30, AND 40 FRAMES COMBINED. THE WIDTH OF THE GAUSSIAN FIT $\sigma_{\text{(data-fit)/fit}}$ GIVES THE PRECISION OF THE MEASUREMENT AND σ_{pull} GIVES THE WIDTH OF THE FIT OF THE PULL DISTRIBUTION WITH STATISTICAL UNCERTAINTIES ONLY. LHC FILL 4449

Frames used	$\sigma_{\text{(data-fit)/fit}}$ (%)		σ_{pull}	
	TPX02	TPX12	TPX02	TPX12
1	0.30	0.30	1.50	1.57
10	0.11	0.12	1.76	1.94
20	0.09	0.10	1.96	2.36
30	0.08	0.09	2.21	2.56
40	0.08	0.09	2.35	2.88

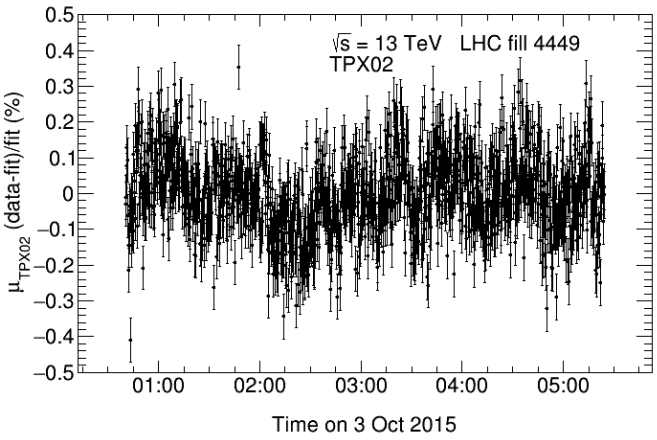

Fig. 6. Relative difference between the data and the fitted average number of interactions per bunch crossing as a function of time, seen by TPX02 averaged over layer-1 and layer-2. The data are shown for the 10 frames (1 s each) combined in order to decrease the statistical uncertainty. LHC fill 4449.

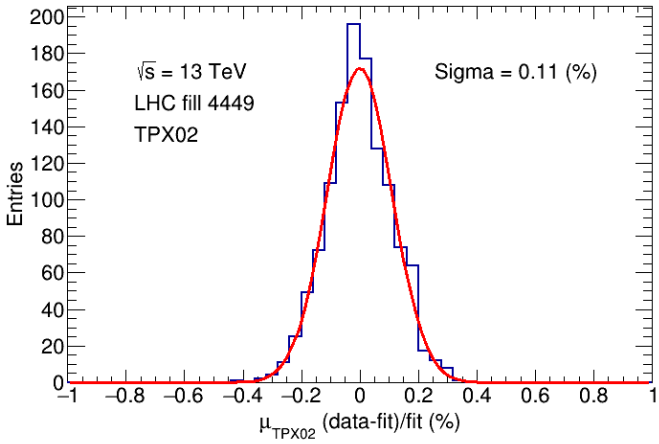

Fig. 7. Gaussian fit of the relative difference between the data and the fitted average number of interactions per bunch crossing as a function of time, seen by TPX02 averaged over layer-1 and layer-2. The data are shown for the 10 frames (1 s each) combined in order to decrease the statistical uncertainty. LHC fill 4449.

the same TPX device is studied as a function of time. The statistical precision is increased by grouping 10, 20, 30, and 40 frames. Fig. 9 shows the fit results for the ten frames

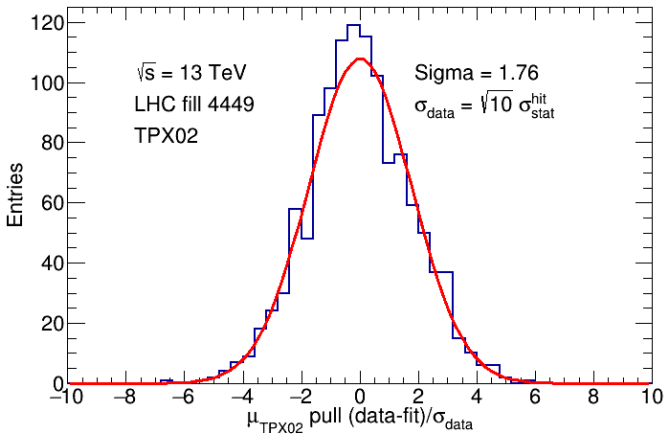

Fig. 8. Pull distribution defined as (data fit)/σ_{data}, where $\sigma_{\text{data}} = \sqrt{R} \cdot \sigma_{\text{stat}}^{\text{hit}}$, with $R = N_{\text{hit}}/N_{\text{cl}} = 10$. The data are averaged over layer-1 and layer-2 for TPX02 and TPX12 with the ten frames (1 s each) combined. The data shown in Fig. 7 are used. LHC fill 4449.

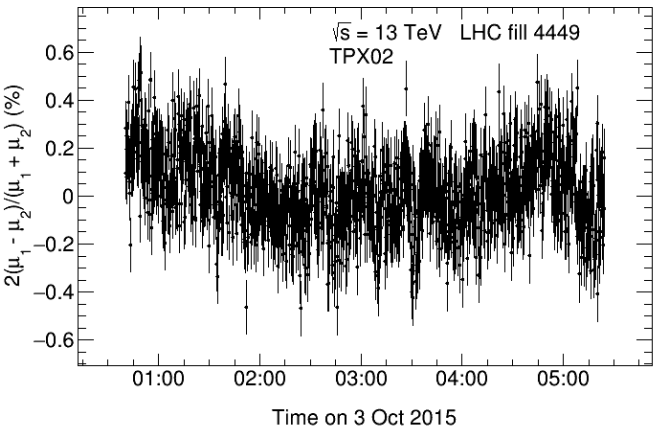

Fig. 9. Relative difference between the average number of interactions per bunch crossing measured by layer-1 and layer-2 of TPX02 as a function of time. The data are shown for the ten frames (1 s each) combined in order to decrease the statistical uncertainty. LHC fill 4449.

combined, while Fig. 10 shows the corresponding precision as the width of the Gaussian fit. The resulting pull distribution is shown in Fig. 11. For single frames, the width of the pull distribution is about unity, indicating that the statistical uncertainty is dominant. The width of the pull distribution is increasing as more frames are combined in order to decrease the statistical uncertainty, and the pull values indicate that in addition systematic uncertainties are present.

Table VII lists the obtained precisions for TPX02 and TPX12. As the difference of two measurements (from layer-1 and layer-2) is calculated and the statistical significance of each measurement is about the same, the uncertainty of each measurement is about $\sqrt{2}$ of overall uncertainty, thus leading to a measurement precision for each TPX device of approximately 0.1% for 10-s time intervals.

VI. LONG-TERM STABILITY OF INDIVIDUAL TPX DEVICES

The long-term time stability of the luminosity monitoring is determined for individual TPX devices by comparing the

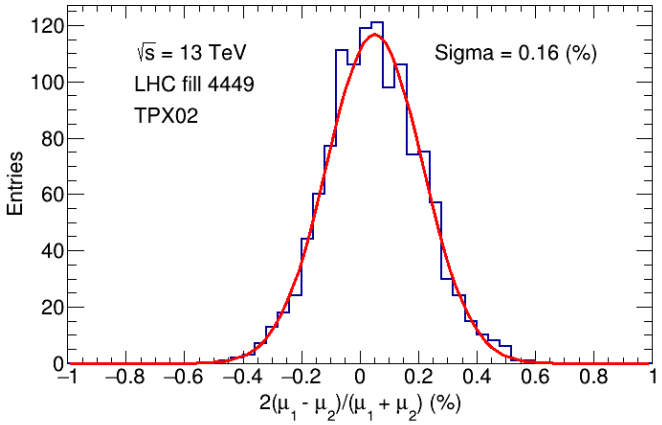

Fig. 10. Gaussian fit of the relative difference between the average number of interactions per bunch crossing measured by layer-1 and layer-2 of TPX02 and TPX12 as a function of time. The data are shown for the ten frames (1 s each) combined in order to decrease the statistical uncertainty. LHC fill 4449.

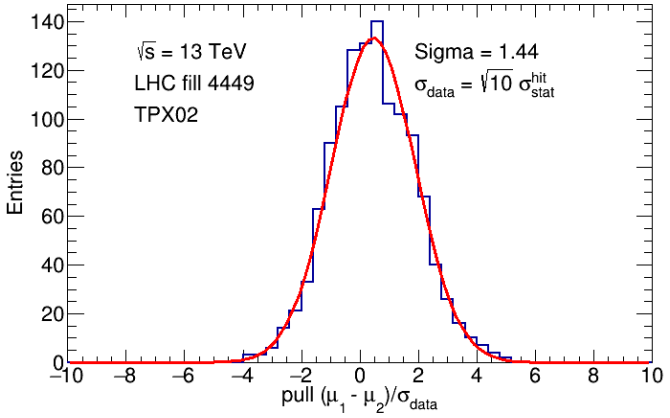

Fig. 11. Pull distribution defined as $(\mu_2-\mu_1)/\sigma_{\text{data}}$, where $\sigma_{\text{data}} = \sqrt{R}\cdot\sigma_{\text{stat}}^{\text{hit}}$, with $R = N_{\text{hit}}/N_{\text{cl}} = 10$ for TPX02. The data shown in Fig. 10 are used. LHC fill 4449.

TABLE VII

PRECISION OF TPX02 AND TPX12 LUMINOSITY MEASUREMENTS BETWEEN LAYER-1 AND LAYER-2. THE PRECISION IS GIVEN FOR 1 FRAME AND FOR 10, 20, 30 AND 40 FRAMES COMBINED. THE WIDTH OF THE GAUSSIAN FIT $\sigma_{2(\mu_1-\mu_2)/(\mu_1+\mu_2)}$ GIVES THE PRECISION OF THE MEASUREMENT AND σ_{pull} GIVES THE WIDTH OF THE FIT OF THE PULL DISTRIBUTION WITH STATISTICAL UNCERTAINTIES ONLY. LHC FILL 4449

Frames used	$\sigma_{2(\mu_1-\mu_2)/(\mu_1+\mu_2)}$ (%) TPX02	TPX12	σ_{pull} TPX02	TPX12
1	0.41	0.41	1.15	1.12
10	0.16	0.17	1.44	1.45
20	0.14	0.14	1.66	1.66
30	0.12	0.13	1.89	2.04
40	0.11	0.13	1.95	2.09

luminosity measured by the two separate sensitive layers of TPX02 and TPX12. For this analysis, the frames are grouped corresponding to time periods of the 2015 LHC fills with instantaneous luminosity above $1000\mu\text{b}^{-1}\text{s}^{-1}$. A linear fit is

TABLE VIII

SLOPE OF TIME HISTORY OF THE LUMINOSITY RATIO MEASURED BY LAYER-1 AND LAYER-2 FOR TPX02 AND TPX12. THE SLOPE VALUES AND THE UNCERTAINTIES ARE GIVEN PER SECOND AND IN PERCENT PER 100 DAYS

TPX	Slope $(10^{-10}\,\text{s}^{-1})$	σSlope $(10^{-10}\,\text{s}^{-1})$	Slope (%/100d)	σSlope (%/100d)
02	−7.06	1.71	−0.61	0.15
12	−4.51	1.62	−0.39	0.14

TABLE IX

SLOPE OF TIME HISTORY OF THE LUMINOSITY RATIO MEASURED BY TPX02 AND TPX12 AVERAGED OVER THE DATA RECORDED BY LAYER-1 AND LAYER-2. THE SLOPE VALUES AND THE UNCERTAINTIES ARE GIVEN PER SECOND AND IN PERCENT PER 100 DAYS

TPX	Slope $(10^{-10}\,\text{s}^{-1})$	σSlope $(10^{-10}\,\text{s}^{-1})$	Slope (%/100d)	σSlope (%/100d)
02/12	0.25	0.89	0.02	0.08

applied to the (TPX layer-1)/(TPX layer-2) luminosity ratio versus time for the August to November 2015 data-taking period, as given in Fig. 12. The slope of the linear fit is taken as a measure of time stability. The uncertainty is obtained from the fit. As the statistical uncertainty of the ratio measurements for the grouped frames is much less than the systematic uncertainties, each ratio is given equal weight in the fit. The obtained slope values and their uncertainties for TPX02 and TPX12 are summarized in Table VIII. The slope shows that the luminosity ratio measured by layer-1 and layer-2 slightly decreases with time. This could indicate a small relative change in sensitivity with time between the thinner and thicker sensors. The time stability of the luminosity measurements between individual layers is about 0.5% per 100 days.

In addition, a study of the internal calibration transfer was performed. As described in Section III, the normalizations of the TPX sensors were performed with a vdM scan using LHC fill 4266 (August 24, 2015 and August 25, 2015) with a peak luminosity of $2.7\mu\text{b}^{-1}\text{s}^{-1}$. In the same LHC fill, the luminosity was kept constant after the vertical and horizontal scans for about 5 h. Using the data of this time period, the (TPX layer-1)/(TPX layer-2) luminosity ratio was determined with TPX02 and TPX12 and found to be in agreement with the ratios at high luminosity within 0.5% uncertainty.

VII. LONG-TERM STABILITY OF DIFFERENT TPX DEVICES

The long-term time stability of the luminosity monitoring is determined for two TPX devices located about 7 m apart at opposite sides of the primary proton–proton interaction point. First, the frames are grouped into luminosity blocks of about 1 min. This grouping of frames is necessary for a comparative study as the start times of the frames are not synchronized between the TPX devices. Then, the luminosity blocks are grouped into time periods corresponding to the LHC fills with

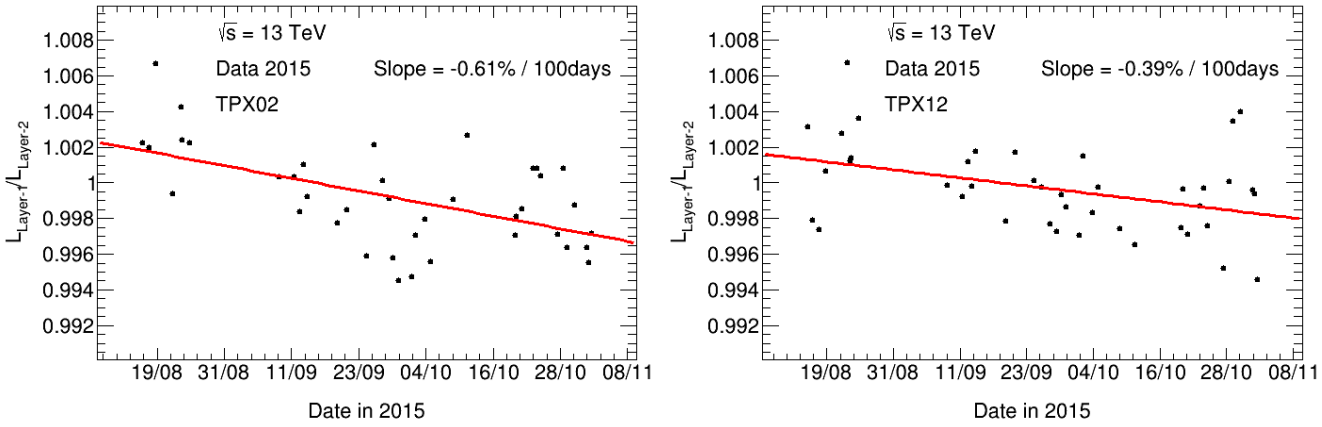

Fig. 12. Time history of the luminosity ratio measured by layer-1 and layer-2 for TPX02 and TPX12. The 2015 TPX data are divided into luminosity blocks of typically 1-min length and then grouped into LHC fill time periods. The size of the statistical error bar is below the size of the data point. A linear fit is applied to determine the slope. LHC fills from August 2015 to November 2015.

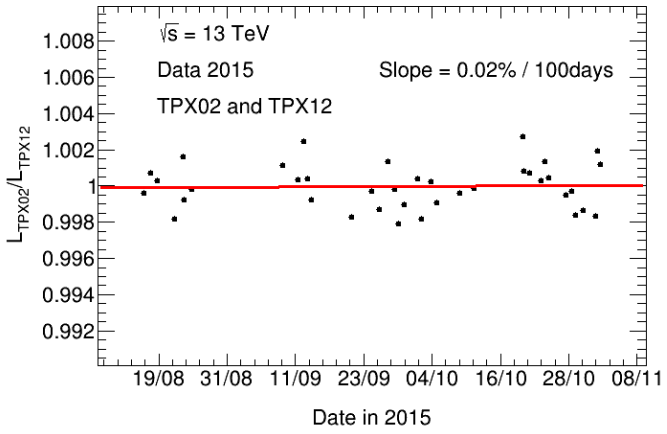

Fig. 13. Time history of the luminosity ratio measured by the TPX02 and TPX12 devices averaged over the data taken by layer-1 and layer-2. The 2015 TPX data are divided into luminosity blocks of typically 1-min length and then grouped into LHC fill time periods. The size of the statistical error bar is below the size of the data point. A linear fit is applied to determine the slope. LHC fills from August 2015 to November 2015.

instantaneous luminosity above $1000\mu b^{-1}s^{-1}$. The luminosity ratio measured by TPX02 and TPX12 is calculated and a linear fit is applied for the August to November 2015 data-taking period, as given in Fig. 13. The slope of the linear fit is taken as a measure of time stability. The obtained slope value and its uncertainty are summarized in Table IX. The uncertainty is obtained from the fit. As the statistical uncertainty of the ratio measurements for the grouped time intervals is much less than the systematic uncertainties, each ratio is given equal weight in the fit. The fluctuations are much larger than the slope of 0.02% per 100 days, and therefore, the largest fluctuations are used as an estimate of the long-term time stability. These fluctuations could either result from the TPX operation or from small variations in the complex LHC radiation field depending on small changes in the colliding beam optics. Thus, conservatively, the study of two different TPX devices indicates an internal time stability of the luminosity measurement below 0.5% per 100 days.

VIII. Conclusion

The network of TPX devices installed in the ATLAS detector cavern has successfully taken data at LHC during Run-2 with 13-TeV proton–proton collisions. An approximate absolute luminosity calibration was determined from a vdM scan in 2015. The TPX network measured the LHC luminosity curve with precision indicating that the luminosity reduction from single-bunch interactions was much less than from beam–beam interactions. The relative short-term precision of the TPX luminosity measurements was determined to be 0.1% for 10-s time intervals, and the internal long-term stability of the TPX system for luminosity measurements was below 0.5% for the 2015 data-taking period.

Acknowledgment

The authors would like to thank the ATLAS Luminosity Group for the useful discussions and interactions and the Medipix Collaboration for providing the TPX assemblies.

References

[1] C. Leroy, S. Pospisil, M. Suk, and Z. Vykydal. (2014). *Proposal to Measure Radiation Field Characteristics, Luminosity and Induced Radioactivity in ATLAS With TIMEPIX Devices, Project Proposal*. [Online]. Available: http://cds.cern.ch/record/1646970

[2] B. Bergmann, I. Caicedo, C. Leroy, S. Pospisil, and Z. Vykydal, "ATLAS-TPX: A two-layer pixel detector setup for neutron detection and radiation field characterization," *J. Instrum.*, vol. 11, no. 10, p. P10002, 2016.

[3] X. Llopart, R. Ballabriga, M. Campbell, L. Tlustos, and W. Wong, "Timepix, a 65k programmable pixel readout chip for arrival time, energy and/or photon counting measurements," *Nucl. Instrum. Methods Phys. Res. A, Accel. Spectrom. Detect. Assoc. Equip.*, vol. A581, nos. 1–2, pp. 485–494, Oct. 2007.

[4] X. Llopart, R. Ballabriga, M. Campbell, L. Tlustos, and W. Wong, "Timepix, a 65k programmable pixel readout chip for arrival time, energy and/or photon counting measurements," *Nucl. Instrum. Methods Phys. Res. A, Accel. Spectrom. Detect. Assoc. Equip.*, vol. A585, pp. 106–108, 2008.

[5] Z. Vykydal *et al.*, "The Medipix2-based network for measurement of spectral characteristics and composition of radiation in ATLAS detector," *Nucl. Instrum. Methods Phys. Res. A, Accel. Spectrom. Detect. Assoc. Equip.*, vol. A607, no. 1, pp. 35–37, Aug. 2009.

[6] M. Campbell *et al.*, "Analysis of the radiation field in ATLAS Using 2008–2011 data from the ATLAS-MPX network," CERN, Geneva, Switzerland, Tech. Rep. ATL-GEN-PUB-2013-001, 2013.
[7] A. Sopczak *et al.*, "MPX detectors as LHC luminosity monitor," *IEEE Trans. Nucl. Sci.*, vol. 62, no. 6, pp. 3225–3241, Dec. 2015.
[8] S. van der Meer, "Calibration of the effective beam height in the ISR," CERN, Geneva, Switzerland, Tech. Rep. ISR-PO/68-31, 1968.
[9] Z. Vykydal *et al.*, "Evaluation of the ATLAS-MPX devices for neutron field spectral composition measurement in the ATLAS experiment," in *Proc. Conf. Rec. IEEE Nucl. Sci. Symp. (NSS)*, Oct. 2008, pp. 2353–2367.
[10] ATLAS Collaboration, "Improved luminosity determination in pp collisions at $\sqrt{s} = 7$ TeV using the ATLAS detector at the LHC," *Eur. Phys. J. C*, vol. 73, no. 8, pp. 2518–2547, 2013.
[11] ATLAS Collaboration, "Luminosity determination in pp collisions at $\sqrt{s} = 8$ TeV using the ATLAS detector at the LHC," *Eur. Phys. J. C*, vol. 76, no. 12, pp. 653–698, 2016.
[12] A. Ball *et al.*, "Design, implementation and first measurements with the medipix2-MXR detector at the compact muon solenoid experiment," *J. Instrum.*, vol. 6, no. 08, p. P08005, 2011.
[13] CMS Collaboration, "CMS luminosity based on pixel cluster counting—Summer 2013 update," CERN, Geneva, Switzerland, Tech. Rep. CMSPAS-LUM-13-001, 2013.
[14] LHC. (2015). *Accelerator Performance and Statistics*, accessed on Mar. 13, 2017. [Online]. Available: http://lhc-statistics.web.cern.ch/LHC-Statistics
[15] ATLAS Collaboration, "Measurement of the inelastic proton-proton cross section at $\sqrt{s} = 13$ TeV with the ATLAS detector at the LHC," *Phys. Rev. Lett.*, vol. 117, no. 18, p. 182002, 2016.
[16] F. Antoniou *et al.*, "LHC luminosity modeling for RUNII," in *Proc. 7th Int. Particle Accel. Conf. (IPAC)*, Busan, South Korea, May 2016, p. 4. [Online]. Available: http://inspirehep.net/record/1469916/files/tupmw002.pdf
[17] K. Eggert, K. Honkavaara, and A. Morsch, "Luminosity considerations for the LHC," CERN, Geneva, Switzerland, Tech. Rep. CERN-AT-94-04, LHC-NOTE-263, 1994.
[18] ATLAS Collaboration, "The ATLAS experiment at the CERN large hadron collider," *J. Instrum.*, vol. 3, p. S08003, Aug. 2008.
[19] CMS Collaboration, "The CMS experiment at the CERN LHC," *J. Instrum.*, vol. 3, no. 8, p. S08004, 2008.